THE ASTROPHYSICAL JOURNAL, 407:752–757, 1993 April 20

LOW-FLUX HARD STATE OF 1E 1740.7−2942

E. CHURAZOV, M. GILFANOV, R. SUNYAEV, M. PAVLINSKY, S. GREBENEV, A. DYACHKOV, V. KOVTUNENKO, AND R. KREMNEV
Space Research Institute, Profsouznaya 84/32, 117810 Moscow, Russia
M. NIEL, P. MANDROU, G. VEDRENNE, AND J. P. ROQUES
Centre d'Etude Spatiale des Rayonnements, 9, avenu du Colonel Roche, BP 4346, 31029 Toulouse Cedex, France
AND
B. CORDIER, A. GOLDWURM, F. LEBRUN, AND J. PAUL
Service d'Astrophysique, Centre d'Etudes Nucleaires de Saclay, 91191 Gif-sur-Yvette Cedex, France
Received 1992 April 20; accepted 1992 October 16

ABSTRACT

GRANAT observations of 1E 1740.7−2942 in 1991 October revealed the source at low 40–150 keV flux level, ∼20–30 mCrab ($\sim\frac{1}{5}$ of the typical 1990 value). The source spectrum in the 150–600 keV energy domain exhibits notable excess above a power-law extrapolation of the lower energy part (4–150 keV) of the spectrum. Comparison of the 1991 October spectrum with the "standard" state spectrum observed in 1990 suggests some analogy with γ_2–γ_1 states transition, observed for the well-known black hole candidate Cygnus X-1 by *HEAO 3* (Ling et al.). Previously a transient high-energy feature, possibly associated with electron-positron annihilation, has been detected in the spectrum of 1E 1740.7−2942 by *GRANAT* on 1990 October 13–14, when 40–150 keV flux was ∼5 times higher than during 1991 fall observations. This indicates that the hardness of the 1E 1740.7−2942 spectrum is not connected with some specific value of X-ray luminosity and mass accretion rate.

During *GRANAT* observations of the source in 1991 August–September the source was below ART-P and SIGMA detection limits, i.e., in the lowest state whenever observed by *GRANAT* in 1990–1991, indicating that the hard X-ray flux is variable by a factor of more than 10 on the time scale of ∼1 yr. On this basis constraints on the parameters of the molecular cloud possibly associated with 1E 1740.7−2942 were derived.

Subject headings: stars: individual (1E 1740.7−2942)

1. INTRODUCTION

The source 1E 1740.7−2942 was intensively studied with the instruments aboard the *GRANAT Observatory* since 1990 March (Sunyaev et al. 1991a). During 1990 spring the source was found to be the brightest source above 35 keV in the vicinity (∼50′) of the Galactic center (GC), with a spectrum similar to that of Cyg X-1 (Sunyaev & Truemper 1979; Nolan et al. 1981) in its "nominal" γ_2 (Ling et al. 1987) state. On this basis it was suggested the source be included in the list of black hole candidates (Sunyaev et al 1991a). The same spectrum was observed in most of the 1990 fall observations except for October 13–14, when a transient high-energy feature was detected in the 200–600 keV energy domain, possibly associated with electron-positron annihilation processes in the source (Sunyaev et al. 1991b; Bouchet et al. 1991). In 1991 spring, the source was found in a low state with a flux at the level of ∼15%–20% of the 1990 average value (Sunyaev et al. 1991b).

A further indication of the source peculiarity came from radio observations (Bally & Leventhal 1991a, b; Mirabel et al. 1991), which revealed a molecular cloud in the source direction. The possible consequences of the presence of cold gas in the vicinity of the compact source were discussed by Bally & Leventhal (1991a, b), Sunyaev et al. (1991b), Mirabel et al. (1991), and Ramaty et al. (1992). Two-point radio sources have been reported close to the position of 1E 1740.7−2942 (Prince & Skinner 1991). Recently, correlation of radio flux from one of these point sources with X-ray flux from 1E 1740.7−2942 and jet-type structures on both sides of it has been discovered by Mirabel et al. (1992). The discovery of jets and the existence of the variable compact source permitted Phinney (1992) to consider 1E 1740.7−2942 as a microquasar and the big accelerator in the vicinity of the GC.

Below we report the results of *GRANAT* observations of 1E 1740.7−2942 during 1991 fall (from August 30 to October 20). During the first month of these observations (till the end of September) the source was below detection limits of ART-P and SIGMA instruments. In October the source was detected by both telescopes with an average 4–150 keV flux at the level of ∼20–30 mCrab with the spectrum being significantly harder than the one observed during 1990 in the "standard" state of the source.

2. INSTRUMENTS AND OBSERVATIONS

The SIGMA coded mask telescope (Paul et al. 1991) with a NaI position sensitive detector (Anger camera principle) provides sky images in the energy range 35–1300 keV with an angular resolution of ∼15′. The instrumental field of view (FOV) at half-sensitivity boundary is a 11°.4 × 10°.5 rectangle. Another coded mask telescope on board *GRANAT*—ART-P (Sunyaev et al. 1990)—operates in the 4–30 keV standard X-ray band and has 3°.4 by 3°.6 FOV (full width at zero response) with nominal angular resolution of ∼5′.

During 1991 fall the source was within the SIGMA FOV on August 30–September 1, September 3, 8, 19, 20–21, 23–24, 24–25, and October 1–2, 2–3, 6–7, 9–10, 10–11, 17–18, and 18–19. ART-P observed the source on August 30–September 1, September 19, 23–24, October 15–16, 17–18, 18–19, 19–20. The

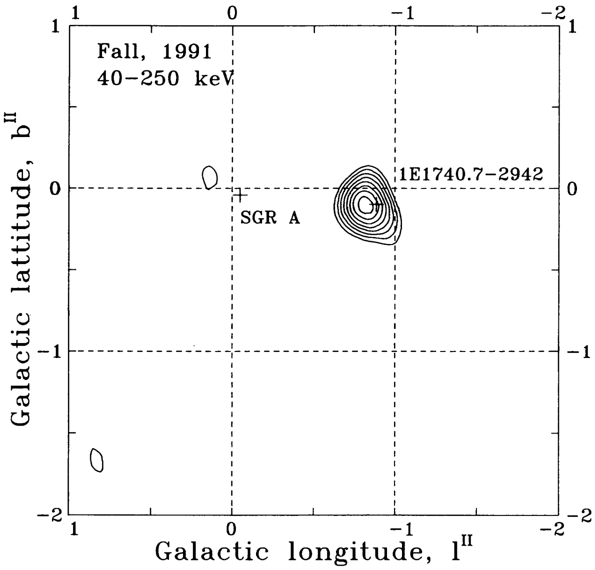

FIG. 1*a*

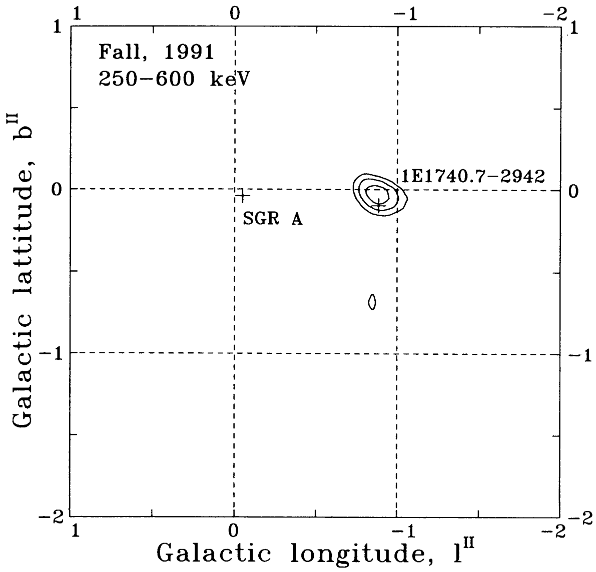

FIG. 1*b*

FIG. 1.—The X-ray maps of the region near the GC, obtained by SIGMA during the observations from 1991 October 1 to October 18 (*a*: 40–250 keV; *b*: 250–600 keV). The total integration time is $\sim 3.3 \times 10^5$ s (corrected for dead time). Contours are 3, 3.5, 4, 4.5 ... σ. At the position of 1E 1740.7−2942, 1 σ corresponds to 4.3 mCrab (40–250 keV) and 47 mCrab (250–600 keV).

duration of SIGMA observations varied from ∼4 hr to ∼40 hr and the ART-P ones lasted typically ∼8 hr. The SIGMA images obtained in the first seven observations (August–September) were contaminated by the presence of the strong hard X-ray source GX 339−4 (Fishman et al. 1991; Sunyaev et al. 1991c) located ∼20° from the center of the FOV. Due to the partial transparency of the material between the passive shields of the telescope, the emission from GX 339−4 produced an arclike structure on the detector, which affects the image quality. A special cleaning procedure was applied to the images, reducing the influence of GX 339−4. A by-product of this procedure was a ∼20% loss in the instrument sensitivity. According to the SIGMA observations of GX 339−4 on September 28, the hard X-ray flux from this source declined by several times as compared with the August level. Therefore the October observations of the GC region were free from this contamination.

3. FALL 1991 IMAGES

The images (SIGMA data) obtained as the sum of the last seven observations (all sessions in 1991 October) in two hard X-ray bands are shown in Figure 1. In order to increase the S/N ratio, the images were convolved with the instrument spatial point-spread function (PSF). The centroids of the peaks (6.8 σ in 40–250 keV band and 4.3 σ in the 250–600 keV band) are located within ∼4′ from the most precise position of 1E 1740.7−2942 obtained by TTM on *MIR*-Kvant (Skinner et al. 1991). Taking into account the moderate significance of the peaks in the SIGMA images, we consider that their positions are compatible with 1E 1740.7−2942. The peaks detected in the ART-P images (standard X-ray band) in each session after October 1 were located with 1′ from 1E 1740.7−2942.

4. FALL 1991 LIGHT CURVE AND SPECTRUM

The light curves of 1E 1740.7−2942 in the 8–20 keV (ART-P data) and 35–300 keV (SIGMA data) energy bands are shown in Figure 2. During the first half of the observations (August 30 through September 25) the source was below the SIGMA detection limit with an upper limit on the average flux in the 35–300 keV band of ∼13 mCrab (3 σ). In each of the seven following observations, the source was detected at a level of ∼2–4 σ with an averaged flux of 27.3 ± 4.1 mCrab (35–300 keV). During the ART-P observations of August 29 through September 23 the source was not detected in the standard X-ray band (3 σ upper limit on the 8–20 keV flux ∼7 mCrab), thus confirming that the source in the standard X-ray band was also in a very low state. In each of the four subsequent ART-P observations, between October 15 through October 20, the source was detected at a flux level of ∼20 mCrab.

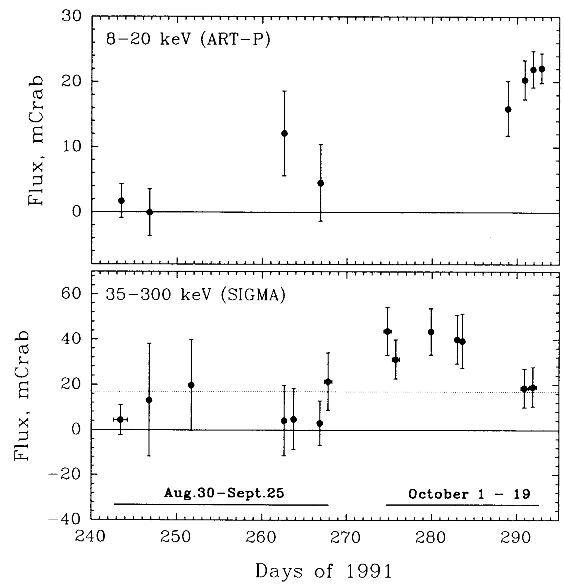

FIG. 2.—Light curve of 1E 1740.7−2942 in the 8–20 keV (ART-P data) and 40–300 keV (SIGMA) bands, obtained by the *GRANAT* during the observations of 1991 fall. Averaged intensity, observed by SIGMA in 1991 spring, is shown in the lower panel by dotted line.

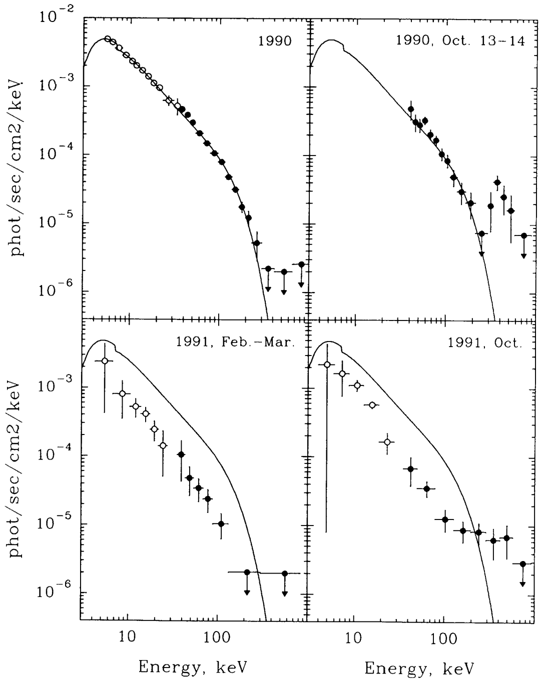

FIG. 3.—Spectra of 1E 1740.7−2942 observed by *GRANAT* during different periods of observations (*filled circles*: SIGMA; *opened circles*: ART-P). Note that ART-P and SIGMA data are not fully contemporary. Solid line shows the Comptonization model approximation of the "standard" state spectrum from Sunyaev et al. (1991b). Points below 1 σ level are replaced with 1 σ upper limits.

In order to increase the statistical significance, the spectra obtained by SIGMA and ART-P in individual sessions starting from October 1 (see Fig. 2) were averaged. The resulting spectrum is shown in Figure 3[1] together with spectra obtained by *GRANAT* during previous observations. Note that the SIGMA and ART-P observations are not fully contemporary. Below 100 keV the spectrum is comparable with that of 1991 spring, but at high energies excess is apparent. The solid line in Figure 3 shows the Comptonization approximation (Sunyaev & Titarchuk 1980) of the "standard" state spectrum with temperature $kT = 33$ keV, half-thickness of the disk $\tau = 1.9$, $N_H = 8 \times 10^{22}$ cm^{-2}. The spectrum of this shape (temperature and optical depth fixed at the values obtained for "standard" state spectrum) cannot fit the 1991 fall data in the 4–1000 keV band: $\chi^2 = 39.5$ for 12 d.o.f. The hardness ratio of the spectrum, defined as ratio of the flux in the 200–600 and 35–200 keV bands $F_{200-600}/F_{35-200} = 0.43 \pm 0.13$, is significantly greater than that of the spectrum averaged over the observations in 1990—$F_{200-600}/F_{35-200} = 0.041 \pm 0.014$. During the hard state, observed on 1990 October 13–14, hardness ratio was $F_{200-600}/F_{35-200} = 0.18 \pm 0.04$.

The 1991 October ART-P and SIGMA data in the 4–150 keV band can be approximated by the power law with low-energy absorption with photon index $\alpha = 2.0 \pm 0.2$ and flux at 100 keV $F_{100} = (1.3 \pm 0.3) \times 10^{-5}$ photons s^{-1} cm^{-2} keV^{-1}, $\chi^2 = 3.2$ for 5 d.o.f. Power-law (with low-energy absorption) approximation in the broad 4–1000 keV range requires $\alpha = 1.8 \pm 0.1$. Although the value of $\chi^2 = 13.8$ for 10 d.o.f. for this fit is acceptable, last four significant points in 150–600 keV band (each point having significance greater than 2 σ) are above the fit. Total significance of the source in 150–600 keV band is ~ 5 σ (or ~ 3.5 σ excess above power law with $\alpha = 1.8$). The SIGMA data only (35–1000 keV) require very hard power law $\alpha = 1.12 \pm 0.25$, $F_{100} = (1.8 \pm 0.3) \times 10^{-5}$ photons s^{-1} cm^{-2} keV^{-1} with $\chi^2 = 5.2$ for 6 d.o.f.

[1] The SIGMA spectra shown in Fig. 3 and Fig. 5 were converted from counts s^{-1} cm^{-2} keV^{-1} to photons s^{-1} cm^{-2} keV^{-1} using the telescope efficiency, calculated for a power-law spectrum with a slope of −2. The same correction has been applied to analytical fits, convolved with response function of the detector. This method is rather accurate for smooth spectra, similar to the "standard" state spectrum of 1E 1740.7−2942, but it may not reproduce the exact spectral shape of more complicated spectra. It was used only for illustration.

5. 1990–1991 HARD X-RAY LIGHT CURVE

The light curve of 1E 1740.7−2942 in the 40–150 keV band, covering almost all SIGMA observations in 1990–1991, is shown in Figure 4. The luminosity of 1E 1740.7−2942 in its different spectral states is given in Table 1, assuming the distance to the source of 8.5 kpc. Solid lines (Fig. 4) at the bottom delimit different states of the source. The arrow points to the observation of 1990 October 13–14, where the transient high-energy feature occurred (note that the 40–150 keV flux in this observation is not distinguishable from the other observations of 1990). Dashed lines in Figure 4 show the level of 120 mCrab ("standard" state observed in 1990) and 16 mCrab ("low" state, average over 1991). The measurements of the 40–150 keV flux from the source in 1991 (18.7 ± 4.0 mCrab averaged over 1991 spring, <13 mCrab [3 σ]—1991 August–September and 22.5 ± 4.1 mCrab—1991 October) are only marginally consistent with the assumption of constant flux during the low state. The χ^2 test, applied to these data, gives a value of $\chi^2 = 7.6$ for 2 d.o.f. which corresponds to a probability of 2.3×10^{-2}. The same test, applied to the 35–300 keV data (13.3 ± 4.0, <13 [3 σ], and 27.3 ± 4.1, respectively, for the same observational periods) gives a value of $\chi^2 = 13.1$ for 2 d.o.f. with associated probability of 1.5×10^{-3}.

6. THE SCATTERING OF THE X-RAYS BY THE MOLECULAR CLOUD

According to Bally & Leventhal (1991b) and Mirabel et al. (1991) there is a molecular cloud (with size $l \sim$ few parsecs and mean density $n_{H_2} \sim 5 \times 10^4$ cm^{-3}) in the direction of 1E 1740.7−2942. Strong low-energy absorption according to observations of SPARTAN (Kawai et al. 1988) and TTM aboard MIR-Kvant (Sunyaev et al. 1991d; Skinner et al. 1991) and weakness of the source in *Einstein* (Hertz & Grindlay 1984) and *ROSAT* (G. Hasinger 1991, private communication) spectral bands is likely due to the location of the source inside or behind the cloud, if there is no strong intrinsic low-energy absorption as observed occasionally in the spectrum of another black hole candidate GS 2023+338 = V404 Cyg (Sunyaev et al. 1991e). Cold gas and the dust in the cloud make easier the explanation of the very narrow annihilation line, detected by germanium experiments from the GC direction. High-density cloud also easily stop jets, as observed by Mirabel et al. (1992).

There are many consequences of the presence of the bright variable X-ray source inside the molecular cloud. One of them was already mentioned in our earlier paper (Sunyaev et al. 1991b). Suppose that the source was in the bright state during several years prior to observation. Due to Compton scattering on the molecules and atoms in the cloud, an additional component should appear with a flux $F_{sc} \sim F_0 \tau_T \sim F_0 l \times 2n_{H_2} \sigma_T$,

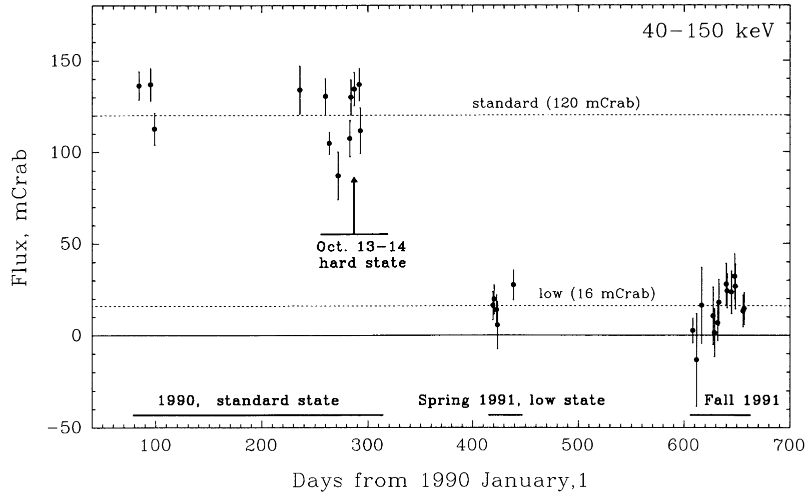

FIG. 4.—The light curve of 1E 1740.7−2942 in the 40–150 keV band, covering almost all SIGMA observations in 1990–1991. Labels mark different states and observational periods. The arrow marks the observation of 1990 October 13–14, when transient high-energy feature has been detected in the spectrum of the source (Sunyaev et al. 1991b). Two dashed lines show the "standard" state (average over 1990) and "low" state (average over 1991) intensity levels.

where F_0 is the flux of the compact source. If the flux of the compact source then declined strongly, a scattered component should remain at the same level during a time $\sim l/c$—the light crossing time of the cloud. It was noted by Sunyaev et al. (1991b) that the low state of 1E 1740.7−2942, observed in 1991 spring, could be explained by such a scattered component.

Note that the angular resolution of the ART-P and SIGMA telescopes corresponds to the linear size of 5–15 parsecs at the distance of the GC. So any emission originating from the cloud even rather far ($\sim$few parsecs) from the compact source would be unresolved by *GRANAT* from the contribution from 1E 1740.7−2942 itself. This refers to the scattered component as well as to the possible positrons annihilation radiation, which could escape from the source neighborhood and annihilate in the cloud (Ramaty et al. 1992).

According to the *GRANAT* observations of 1991 fall, brightening of the source on a time scale of days (Fig. 2) indicates that the observed emission (October 1–19) is related to the compact source itself. On the other hand, the absence of the source during August 30–September 24 allows one to restrict the parameters of the cloud. Indeed, according to the *GRANAT* observations, the source was in a bright state in 1990 (Fig. 4), while $\sim$1 yr later it was below the SIGMA detection limit (August 30–September 24). Using 13 mCrab as the 3 σ upper limit for F_{sc} in the 40–150 keV band from these observations and $\sim$120 mCrab in the same band as F_0

TABLE 1

FLUXES AND LUMINOSITIES OF 1E 1740.7−2942 IN DIFFERENT SPECTRAL STATES, CALCULATED ASSUMING POWER-LAW SPECTRUM WITH PHOTON INDEX 2.1

Parameter	8–20 keV	35–100 keV	100–300 keV	300–600 keV
		1990 Spring–Fall		
F[a]	$(22.0 \pm 0.4) \times 10^{-3}$	$(1.41 \pm 0.04) \times 10^{-2}$	$(4.7 \pm 0.3) \times 10^{-3}$	$(0.3 \pm 0.4) \times 10^{-3}$
L[b]	$(3.96 \pm 0.09) \times 10^{36}$	$(1.09 \pm 0.03) \times 10^{37}$	$(10.5 \pm 0.8) \times 10^{36}$	$(0.2 \pm 0.3) \times 10^{37}$
		1990 Oct 13–14		
F	...	$(1.72 \pm 0.12) \times 10^{-2}$	$(4.4 \pm 0.8) \times 10^{-3}$	$(7.3 \pm 1.5) \times 10^{-3}$
L	...	$(1.33 \pm 0.09) \times 10^{37}$	$(9.9 \pm 1.8) \times 10^{36}$	$(4.1 \pm 0.8) \times 10^{37}$
		1991 Feb 22–Mar 14		
F	$(6.5 \pm 1.5) \times 10^{-3}$	$(2.8 \pm 0.5) \times 10^{-3}$	$(-0.4 \pm 0.3) \times 10^{-3}$	$(-0.7 \pm 0.6) \times 10^{-3}$
L	$(1.3 \pm 0.2) \times 10^{36}$	$(2.1 \pm 0.4) \times 10^{36}$	$(-0.9 \pm 0.8) \times 10^{36}$	$(0.4 \pm 0.4) \times 10^{37}$
		1991 Aug–Sep		
F	$(2.1 \pm 2.1) \times 10^{-3}$	$(0.4 \pm 0.6) \times 10^{-3}$	$(0.4 \pm 0.4) \times 10^{-3}$	$(0.8 \pm 0.7) \times 10^{-3}$
L	$(0.4 \pm 0.3) \times 10^{36}$	$(0.3 \pm 0.4) \times 10^{36}$	$(0.9 \pm 0.8) \times 10^{36}$	$(0.5 \pm 0.4) \times 10^{37}$
		1991 Oct		
F	$(7.4 \pm 0.9) \times 10^{-3}$	$(2.2 \pm 0.5) \times 10^{-3}$	$(1.7 \pm 0.3) \times 10^{-3}$	$(1.9 \pm 0.6) \times 10^{-3}$
L	$(1.3 \pm 0.15) \times 10^{36}$	$(1.7 \pm 0.4) \times 10^{36}$	$(3.9 \pm 0.8) \times 10^{36}$	$(1.1 \pm 0.4) \times 10^{37}$

[a] F: flux in photons $cm^{-2}\ s^{-1}$.

[b] L: luminosity in ergs s^{-1} (for 8.5 kpc distance).

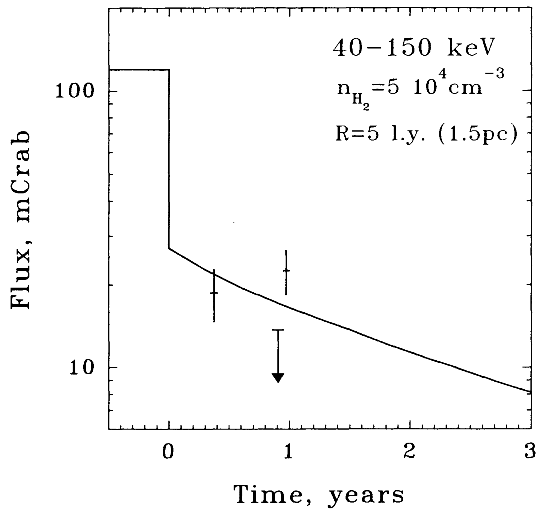

FIG. 5.—Evolution of scattered component 40–150 keV flux after switch-off of the compact source. The source was supposed to be at the center of the cloud. Three data points are the measurements of 40–150 keV flux by SIGMA on 1991 February 22–March 14, August 30–September 25 (3 σ upper limit) and October 1–19.

(averaged value observed in 1990), one can obtain $\tau < 0.1$ ($n_{H_2} l < 8 \times 10^{22}$ cm^{-2}). For the uniform cloud of 1.5 pc radius it means that $n_{H_2} \leq 2 \times 10^4$ cm^{-3}. More accurate calculations of the 40–150 keV flux behavior under one scattering approximation (Fig. 5) gives an upper limit of $n_{H_2} \leq 3 \times 10^4$ cm^{-3}. An alternative explanation of flux decline below the detection limit is the assumption that the lifetime of the scattered component is less than 1 yr. This assumption would require notably smaller size of the cloud than that found by Bally & Leventhal (1991b) and Mirabel et al. (1991).

The spectra of scattered component are shown in Figure 6. The difference with the compact source spectrum is most apparent in the standard X-ray band due to (*a*) the strong absorption at low energies and at the K-edge (7.1 keV) of neutral iron and (*b*) strong 6.4 keV neutral iron fluorescence line (Fig. 6). Of course the 6.4 keV line should also be present during the bright state of the source, but in the scattered component, due to the drop of the continuum level, its equivalent width should increase by a factor $\sim 1/\tau \sim 3$–10. Note also that the equivalent width of 6.4 keV line in the scattered component $W \approx 1$ keV is practically independent on the parameters of the cloud and compact source. Astro-D mission will have enough sensitivity and spectral resolution to prove the location of 1E 1740.7−2942 inside the cloud or at least set strong constraints on its parameters. At energies well above 150 keV the scattered component should also differ from the compact source spectrum due to the recoil effect and decrease of the Klein-Nishina cross section.

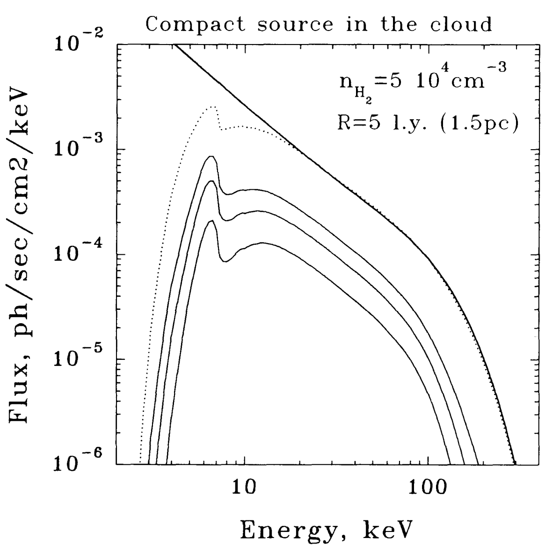

FIG. 6.—Spectra of scattered component calculated under one scattering approximation. *Thick solid line*: assumed spectrum of compact source (Comptonization model); *dotted line*: sum of scattered component and emergent spectrum of the source; *thin solid lines*: scattered component 0, 1, and 3 yr after the compact source switch-off. Note that 6.4 keV line has been added to the spectra as the Gaussian line with FWHM = 0.64 keV.

Note the following important assumptions done for simplicity.

1. It was assumed that before the source switch-off it was persistently bright for several years. This assumption was based on the observations of *GRANAT* in 1990 and *MIR*-Kvant in 1988 (Sunyaev et al. 1991d; Skinner et al. 1991). *GRANAT* and *MIR*-Kvant data cover only a small part of this period and we do not know the 1E 1740.7−2942 flux in between. The date of the compact source turnoff is also known with an accuracy of ~half a year.

2. The nonuniform distribution of gas in the cloud and location of the compact source on the boundary or even outside the cloud will change strongly the simple estimates given above.

The variability of 40–150 keV flux from 1E 1740.7−2942 in low state during 1991 (see also Pavlinsky et al. 1992 for variability in the standard X-ray band) indicates that likely most of the emission observed by *GRANAT* is not related to a scattered component, but originates from the compact source. The observed fluxes (or upper limits) can be nevertheless interpreted as the upper limits on the intensity of the scattered component. Thus the simplest model with the compact source in the center of the cloud shows that weak 40–150 keV flux observed in 1991 August–September gives additional constraints on the cloud parameters or indicates that the source is located rather far from the cloud center.

7. DISCUSSION

The behavior of 1E 1740.7−2942 in hard X-rays resembles that of one of the most plausible Galactic black hole candidates, Cygnus X-1. Both sources exhibit apparent spectral and intensity changes on the time scale of several months and have analogous "standard" spectra (Sunyaev et al. 1991b). Because of this similarity it is likely that 1E 1740.7−2942 is a binary system like Cyg X-1. The long-term intensity and spectral changes of these two sources could be related with long-term variability of the companion star.

Regarding the low state of 1E 1740.7−2942 (*GRANAT* data in 1991) one could look for some analogy in Cyg X-1 data. The flux at 100 keV from Cyg X-1 declines several times with respect to nominal γ_2 value either during soft (high) or hard γ_1 states (Ling et al. 1987). In the soft state, a drop of 100 keV flux was accompanied by the appearance of a bright blackbody component with $kT \sim 1$–2 keV. The spectrum of such a shape would contradict ART-P data in 1991 unless the blackbody temperature is several times lower and the soft component is almost completely absorbed by neutral gas on the line of sight ($N_H \sim 10^{23}$ cm^{-2}). In the γ_1 state the excess at ~MeV energies appeared simultaneously with 100 keV flux decline. Due to the larger distance of 1E 1740.7−2942 the presence of ~MeV excess (analogous in luminosity to γ_1 state of Cyg X-1) would not be detectable by SIGMA. Although the excess in the spectrum of 1E 1740.7−2942 in 1991 fall was observed at notably lower energies (~200–600 keV) it could indicate that the low state of 1E 1740.7−2942 is similar to some extent to the γ_1 state of Cyg X-1. Note, however, that previously the high-energy bump in the spectrum of 1E 1740.7−2942 was detected on 1990 October 13–14 (see Fig. 3), when 35–600 keV luminosity was ~4 times higher than that of 1991 October. This indicates that the appearance of high-energy excesses is not related to one specific value of the hard X-ray flux (or mass accretion rate if most energy is emitted in X-rays).

Due to relatively poor statistics of high-energy points of 1991 October spectrum, various models, which include an excess in the 200–600 keV band, can fit these data better than a simple power law. Assuming a two-component spectrum (i.e., low-energy power law + hard component) and fixing the slope and normalization of the power law at 4–150 keV best fit values ($\alpha = 2.0$, $F_{100} = 1.3 \times 10^{-5}$ photons s^{-1} cm^{-2} keV^{-1}), one can estimate the required parameters of hard component (see below).

The χ^2 calculated for the low-energy power law (Fig. 7) over a broad range 4–1000 keV is equal to 16.4 for 13 data points. Adding of the Wien component with $kT \sim 150$ keV (Fig. 7), which could arise from the hot optically thick region of the disk, reduces the value of χ^2 to 4.9.

In relation with the cold molecular cloud possibly surrounding the source (Bally & Leventhal 1991a, b; Mirabel et al. 1991), a model with positronium annihilation spectrum might be important. The molecular cloud rich of cold gas could be an appropriate site for deceleration and cooling of hot positrons which were born in the vicinity of the compact source and then escaped. A low-energy power law plus a positronium annihilation spectrum consisting of a narrow 511 keV line and a three-photon continuum ($F_{511} = 5.1 \times 10^{-4}$ photons s^{-1} cm^{-2}, positronium fraction fixed at 1, $\chi^2 = 3.1$) is shown in Figure 6. A crucial test for attributing the observed excess to the electron-positron annihilation via positronium formation could be the presence of a narrow 511 keV line. Unfortunately, the 511 keV line flux required by the positronium annihilation model is below the SIGMA sensitivity to narrow 511 keV line, achieved during these observations $\sim 1.6 \times 10^{-3}$ photons s^{-1} cm^{-2} (3 σ). The flux actually detected within the FWHM of the 511 keV line has a significance of 1.1 σ and neither contradicts nor supports the positronium annihilation scenario.

The hot pair cloud model has been discussed by Ling et al. (1987) and Liang & Dermer (1988) as the explanation of the MeV excess in the γ_1 state of Cyg X-1. Using simplest approximation of the annihilation spectrum of hot, optically thin electron-positron plasma as Gaussian line (Ramaty & Meszaros 1981; Aharonian, Atoyan, & Sunyaev 1983), one can expect the annihilation component in the spectrum as a bump at the energy of the order or higher than 511 keV. As the temperature of the annihilating particles increases, the bump is shifting to higher energies and becoming broader. It is therefore unlikely that 200–600 keV bumps observed by SIGMA from 1E 1740.7−2942 (1990 October 13–14 and 1991 October 1–19) can be directly explained by annihilating spectrum of hot positrons, since the bulk flux in excesses is below 500 keV. Such models require the unusually high gravitational redshifts ~0.8 (in order to shift the excess to lower energies) and rather low temperatures of annihilating particles: $\sim 5 \times 10^8$ K for 1990 October 13–14 and $\sim 1.2 \times 10^9$ K for 1991 October 1–19 ($\chi^2 = 5.5$).

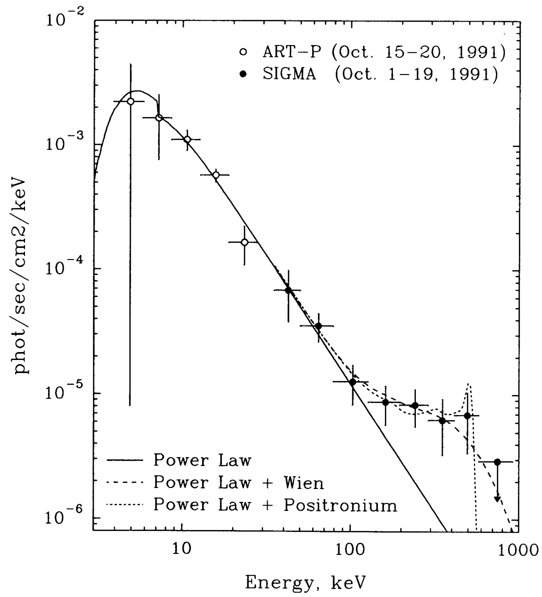

FIG. 7.—Spectrum of 1E 1740.7−2942 averaged over observations from 1991 October 1 to 19. The following approximations are shown: *solid line*: power law fit to low-energy (4–150 keV) points with $\alpha = 2.0$; *dotted line*: low-energy power law plus Wien component with $kT = 150$ keV; *dashed line*: low-energy power law plus positronium annihilation spectrum with flux in narrow line 5.1×10^{-4} photons s^{-1} cm^{-2}. Points below 1 σ level are replaced with 1 σ upper limits.

We are grateful to an anonymous referee for useful comments and suggestions. E. Churazov and M. Gilfanov acknowledge the support by grant of American Astronomical Society.

REFERENCES

Aharonian, F., Atoyan, A., & Sunyaev, R. 1983, A&SS, 93, 229
Bally, J., & Leventhal, M. 1991a, IAU Circ., No. 5252
———. 1991b, Nature, 353, 234
Bouchet, L., et al. 1991, ApJ, 383, L45
Fishman, G., Wilson, R., Meegan, C., Harmon, A., & Brock, M. 1991, IAU Circ., No. 5327
Hertz, P., & Grindlay, J. E. 1984, ApJ, 278, 137
Kawai, N., et al. 1988, ApJ, 330, 130
Liang, E. P., & Dermer, C. D. 1988, ApJ, 325, L39
Ling, J. C., Mahoney, W. A., Wheaton, W. A., & Jacobson, A. S. 1987, ApJ, 241, L117
Mirabel, I. F., Morris, M., Wink, J., Paul, J., & Cordier, B. 1991, A&A, 251, L43
Mirabel, I. F., Rodriguez, L. F., Cordier, B., Paul, J., & Lebrun, F. 1992, Nature, 358, 215
Nolan, P., Gruber, D. E., Knight, F. K., Matteson, J. L., Rotschild, R. E., Marshall, F. E., Levine, A. M., & Promini, F. A. 1981, Nature, 293, 275
Paul, J., et al. 1991, in Adv. Space Res., 11, (8), 289
Pavlinsky, M., et al. 1992, Soviet Astron. Lett., in press
Phinney, E. S. 1992, Nature, 358, 189
Prince, T., & Skinner, G. 1991, IAU Circ., No. 5228.
Ramaty, R., Leventhal, M., Chan, K., & Lingenfelter, R. 1992, ApJ, 392, L63
Ramaty, R., & Meszaros, P. 1981, ApJ, 250, 384
Skinner, G. K., et al. 1991, A&A, 252, 172
Sunyaev, R., Babichenko, S., Gaganov, D., Tabaldyev, C., & Yamburenko, N. 1990, Adv. Space Res., 10, (2), 233
Sunyaev, R., Churazov, E., & Gilfanov, M. 1992, in preparation
Sunyaev, R., et al. 1991a, A&A, 247, L29
Sunyaev, R., et al. 1991b, ApJ, 383, L49
Sunyaev, R., Gilfanov, M., Goldwurm, A., & Schmitz-Fraysse, M. C. 1991c, IAU Circ., No. 5342
Sunyaev, R., et al. 1991d, Soviet Astron. Lett., 17, 126
Sunyaev, R., Kaniovsky, A., Efremov, V., et al. 1991e, Soviet Astron. Lett., 17, 291
Sunyaev, R., & Titarchuk, L. 1980, A&A, 86, 121
Sunyaev, R., & Truemper, J. 1979, Nature, 279, 506